

Article

Latin Hypercube Sampling Method for Location Selection of Multi-Infeed HVDC System Terminal

Xiangqi Li ^{1,2}, Yunfeng Li ², Li Liu ³, Weiyu Wang ³, Yong Li ^{3,*}  and Yijia Cao ³

¹ College of Electrical and Information Engineering, Changsha University of Science and Technology, Changsha 410004, China; lixq@hn.sgcc.com.cn

² State Grid Hunan Electric Power Company Limited Economic & Technical Research Institute, Changsha 410004, China; liyunfeng@geiri.sgcc.com.cn

³ College of Electrical and Information Engineering, Hunan University, Changsha 410082, China; liuli1995@hnu.edu.cn (L.L.); victor0125@hnu.edu.cn (W.W.); yjcao@hnu.edu.cn (Y.C.)

* Correspondence: yongli@hnu.edu.cn

Received: 26 February 2020; Accepted: 26 March 2020; Published: 2 April 2020



Abstract: Owing to the stochastic states of power systems with large-scale renewable generation, the impact of high-voltage direct current (HVDC) systems on the stability of the power system should be examined in a probabilistic manner. A probabilistic small signal stability assessment methodology to select the best locations for multi-infeed high-voltage direct current systems in alternating current (AC) grids is proposed in this paper. The Latin hypercube sampling-based Monte Carlo simulation approach is taken to generate the stochastic operation scenarios of power systems with the consideration of several stochastic factors, i.e., load demand and power generation. The damping ratio of the critical oscillation modes and the controllability of power injection to oscillation modes are analyzed by the probabilistic small signal stability. A probabilistic index is proposed to select the best locations of high-voltage direct current systems for improving the damping of the oscillation modes. The proposed methodology is applied to an IEEE 39 bus system considering the stochastic load demand and power generation. The results of probabilistic small signal stability assessment and a time-domain simulation show that the installation of a high-voltage direct current system on the selected locations can effectively improve the system damping.

Keywords: HVDC placement; probability stability; modal analysis; Monte Carlo simulation; Latin hypercube sampling

1. Introduction

With the progress of power systems, especially the extension of large-scale interconnected power systems, the inter-area oscillation issue is becoming a major problem. The weak connection between subsystems may cause oscillation issues of the interconnected power system, particularly during the initial period of the interconnected power system. High-voltage direct current (HVDC) transmission systems are a promising method to enhance the connection of the interconnected power systems. The integration of HVDC systems makes the structure of the receiving-side power systems more complex. Moreover, the large-scale renewable generation can be integrated by HVDC systems, which increases the uncertainties of the system operation states. Thus, the location of HVDC, especially multi-infeed HVDC systems, on the system security and stability should be examined carefully [1,2].

Different methods have been proposed to investigate the best placement of HVDC converters. Most of the methods focus on the optimal power flow with the integration of HVDC power systems. In [3], an optimization algorithm is proposed to identify the HVDC line placement for the relief of congestion of transmission lines and saving the operational cost of the whole system. The trade-off

between the minimization of operational cost and the controllability of the power flow is discussed in [4]. A comprehensive algorithm based on the flexibility matrix is proposed to determine the location of HVDC converters for balancing the cost and flexibility. In [5], the $N-1$ criterion is considered in the location selection of HVDC systems in meshed power systems to reduce the congestion. The problem is transferred to a mixed integer linear programming optimization problem and an adaptive approach is employed to improve the flexibility of the proposed method in large-scale power systems. With the penetration of renewable energy in power systems, the uncertainty of the system operational point is increased, which should be taken into account in the placement of HVDC. In [6], a double stage stochastic optimal algorithm is proposed to deal with uncertainties of load demand and power generation in a HVDC placement problem. The proposed method can find the best HVDC locations for minimizing the load of transmission lines without requiring many parameters. In [7,8], the multi-infeed short-circuit ratio (MISCR) defined by International Council on Large Electric systems (CIGRE) is used to identify the appropriate location of HVDC systems to improve the security of hybrid alternating current/direct current (AC/DC) power systems. However, the aforementioned papers did not consider the impact of HVDC locations on system stability, e.g., the oscillation issues.

Small signal stability analysis (SSSA) is a promising method to investigate the system stability. The conventional SSSA is based on the linearized model and the eigenvalue analysis method of the system is performed at a certain operating point, which belongs to deterministic stability analysis. To examine the stability of a system under different operating conditions, a great number of deterministic states need to be analyzed [9]. The main problem of the deterministic method is that it cannot objectively reflect the inherent uncertainty nature of the system's network structure, power-generation mode, load level and element parameters. Therefore, it is difficult to comprehensively and accurately evaluate the overall system stability [10].

In 1978, Burchett applied the probability method to power system probabilistic small signal stability analysis (PSSSA) for the first time and analyzed the influence of uncertainty of system parameters following normal distribution on the stability of power systems in the case of small disturbance [11]. PSSSA refers to considering the uncertainty of input random variables, conducting SSSA on the power system, and using the probabilistic analysis method to obtain the probabilistic characteristics of the eigenvalues of the electromechanical mode. A quasi-Monte Carlo-based PSSSA method to evaluate the dynamic performance of electric vehicles and energy conversion systems is presented in [12]. A PSSSA method based on Monte Carlo (MC) approach for iterative assessment is proposed in [13] and the PSSSA considers the uncertainties of the operational states by modal analysis of small signal stability. Cumulative probability density function of damping ratios of oscillatory modes (OMs) is used as the evaluation index.

MC simulation is a statistical test method of parameter estimation when the sample size is large. MC has been widely used in power systems such as reliability assessment, and the number of tests has nothing to do with the scale of the system. MC is used to produce a great deal of random computational scenarios in accordance with the distribution density of the random sources [14]. Recent literature has used MC simulation for SSSA of power systems with small sets of random input variables [13,15]. Latin hypercube sampling (LHS) was first proposed by McKay et al. [16] in 1979. It is an efficient stratified sampling technique and it can obtain an accurate result with a much smaller sample size than simple random sampling (SRS) [17].

Owing to the multiple stochastic factors of interconnected power systems, e.g., load demand and power generation, the damping ratio of the OMs may vary with the change of operating states. The Latin hypercube sampling-based Monte Carlo simulation (LHS-MCS) can be used to identify the critical OMs and the locations for the DC system terminal. This paper proposes a PSSSA methodology to evaluate the best location for multi-infeed HVDC systems. The LHS-MCS approach is adopted to generate the stochastic operation scenarios of power systems with the consideration of several stochastic factors, i.e., load demand and power generation. The damping ratio of the critical OMs and the controllability of power injection to OMs are analyzed by the probabilistic small signal stability.

A probabilistic index is proposed to select the best locations of HVDC systems for improving the damping of the OMs. The proposed methodology is tested on an IEEE 39 bus system by selecting the stochastic load demand and power generation. The results of PSSSA and the time-domain simulation show that the installation of the HVDC system on the selected locations can effectively improve the system damping.

The organization of this paper is as follows. Section 2 describes the theoretical background of uncertainty analysis, MC simulation, and the LHS method. Section 3 presents the proposed methodology and discusses the main issues associated with the conditions for application of LHS method in PSSSA and the calculation of probabilistic indices for selecting the best locations of multi-infeed HVDC systems. In Section 4, the selection results of the multi-infeed HVDC systems obtained from a New England 39 bus system are shown. In Section 5, comparisons and discussions with the results of other papers are given. Finally, Section 6 concludes the paper.

2. Theoretical Background

An HVDC system is a promising technique for renewable energy integration. With the increasing penetration of renewable energy integrated by HVDC systems, the operational point of whole power systems is time varying. The stability of hybrid AC/DC power systems could be influenced by the uncertainty originating from the load demand and power generation. In the planning stage of an HVDC system, the influence of HVDC station locations on the system stability must be investigated in a probabilistic way. To analyse the probabilistic stability of hybrid AC/DC power systems and evaluate the candidate locations of HVDC stations, the Monte Carlo method is employed to obtain the random operational scenarios and Latin Hypercube sampling method is used to improve the calculation efficiency.

2.1. Uncertainty Analysis Method

The general physical process of a system can be represented by establishing one physical model. This physical model can usually use an abstract function to represent input and output, and there is a certain mapping relationship, the function is described as:

$$p = h(q) \quad (1)$$

where the vector h is a set of functions describing the behavior of the model, such as the dynamic behavior of power system; $q = [q_1, q_2, \dots]^T$ is a vector of input variables; and $p = [p_1, p_2, \dots]^T$ is a vector of output variables.

From the perspective of probability theory, uncertainty analysis includes determination of the probability density function (PDF) of the output variable p generated by the function h and the PDFs defining the probability space of the input variable q . In addition, the PDF of the output variable p can be represented as a cumulative probability density function (CPDF). Both of the functions summarize the uncertainty of output variables, and yet CPDF provides more illustrative abstracts in sample-based studies. CPDF is formally defined by integration [13]

$$\text{prob}(p_i \leq P) = 1 - \int_{-\infty}^{+\infty} \varphi[h(q)]\text{PDF}(q)dq \quad (2)$$

where $\text{prob}(p_i \leq P)$ is the probability that an output p_i under P will happen, $\text{PDF}(q)$ is the PDF of input variables, the differential dq is the integration domain, and:

$$\varphi[h(q)] = \begin{cases} 1 & \text{if } h(q) > P \\ 0 & \text{if } h(q) \leq P \end{cases} \quad (3)$$

In fact, the integral (2) is obtained by some approximate procedure. Although there are some new methods have been proposed in other literature to Equation (2), the effectiveness of MC simulation in uncertainty evaluation has been proved in many fields [18,19].

2.2. Monte Carlo Simulation

MC simulation aims at estimating the probability of an event by a lot of experiments. The basic thought is firstly to establish a probabilistic model for the problem. The next step is to calculate the statistical characteristics of the problem through a large number of sampling experiments. The final step is to get all kinds of estimators to find the approximate answer.

The application of MC in uncertainty analysis is justified by two statistical theories: (1) the Law of Large Numbers, and (2) the Central Limit Theorem.

Let X_1, X_2, \dots, X_k be a sequence of independent and identically distributed random variables with expectation $E(X_k) = \mu$ ($k = 1, 2, \dots, n$). The arithmetic mean of n variables is calculated by:

$$\bar{X} = \frac{1}{n} \sum_{k=1}^n X_k \quad (4)$$

For any small value $\varepsilon > 0$, the Law of Large Numbers states that:

$$\lim_{n \rightarrow \infty} P(|\bar{X} - \mu| \geq \varepsilon) = 0 \quad (5)$$

Equation (4) indicates that the sampling average of X_k approaches converge in probability towards the expected value μ when n is large enough.

The distribution of the sample average can be described by the Central Limit Theorem. Assume that the variance of X_k is σ^2 ($0 < \sigma^2 < \infty$). For any real number x , the distribution function $F_n(x)$ of sample average is calculated by:

$$\lim_{n \rightarrow \infty} F_n(x) = \lim_{n \rightarrow \infty} P\left(\frac{\bar{X} - \mu}{\sigma / \sqrt{n}} \leq x\right) = \int_{-\infty}^x \frac{1}{\sqrt{2\pi}} e^{-\frac{t^2}{2}} dt = \phi(x) \quad (6)$$

where $\phi(x)$ is the standard normal distribution. When n is large enough, the average of the samples is similar to the normal distribution whose expectation is μ and the variance is σ^2 .

2.3. Latin Hypercube Sampling

LHS is an effective probabilistic sampling method which can be used to generate the necessary scenarios for PSSSA. X_1, X_2, \dots, X_M is the M input random variables. Each random variable obeys a certain probability distribution:

$$Y_m = F_m(X_m). \quad (7)$$

where Y_m is the probability of X_m and is scaled from 0 to 1, and F_m is the probability cumulative function of X_m . The cumulative curve is divided into N equal intervals and only one sampling value should be selected randomly in each interval, which is illustrated in Figure 1.

Then the n th sample value of the m th random variable x_{mn} is calculated by the inverse function of F_m :

$$x_{mn} = F_m^{-1}\left(\frac{n-a}{N}\right) \quad (8)$$

where a is an internal variable which meets the 0–1 distribution. The sample values of X_m can be written in a column vector as $[x_{m1} \ x_{m2} \ \dots \ x_{mN}]^T$. All the sample values of input variables construct a $N \times M$ sampling matrix. Then each column of the sampling matrix should be shuffled randomly, and each row constitute a random scenario [20].

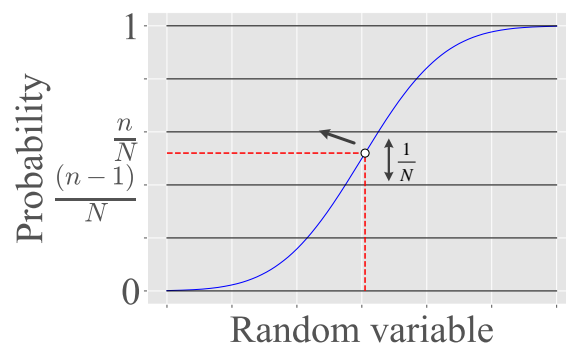


Figure 1. Sampling process of Latin hypercube sampling (LHS).

LHS can effectively improve the computation efficiency of MC as the sampling number are reduced significantly without the loss of accuracy.

3. Proposed Method

3.1. Probabilistic Small Signal Stability Analysis

PSSSA can evaluate the dynamic performance of power systems considering uncertainty operation states. The stochastic operation scenario of power systems are generated firstly, and then the SSSA is used for each of the random scenarios. The probabilistic dynamic characteristics of power systems can be acquired by the probability statistics method, such as distribution of eigenvalues, expectation and variance of damping ratio and oscillation frequency, etc.

The linearized model and the random variables of power systems are the bases of PSSSA. The state matrix A of large-scale complex power systems is obtained by DIGSILENT/PowerFactory, and the input matrix B and output matrix C is obtained by a numerical calculation method introduced in [21].

Several stochastic variables can affect the operation states of power systems, which leads to different distributions of eigenvalues. Random scenarios are composed of different combinations of stochastic variables. In this paper, the following random variables are considered: (1) the output power of synchronous generators; (2) the load demand. Both stochastic variables obey the normal distribution. Then the oscillation characteristics of power systems are analyzed by the statistical method and the location which has the best controllable performance will be distinguished.

3.2. Modal Analysis

The dynamic behavior of one power system is often represented by a series of non-linear ordinary differential equations [22]:

$$\dot{x}_i = f_i(x_1, x_2, \dots, x_n; u_1, u_2, \dots, u_r; t), i = 1, 2, \dots, n \quad (9)$$

where x is the state variables; x_i is a element of the state vector; u_i is the system input variables, which are external signals that can influence the behavior of the system; \dot{x} is the derivative of the state variable with respect to time; n is the system order, r is the number of inputs to the system; and t is time. Equation (9) can be rewritten as follows:

$$\dot{x} = f(x, u, t) \quad (10)$$

where $x = [x_1, x_2, \dots, x_n]^T$ is the state vector; $u = [u_1, u_2, \dots, u_r]^T$ is the input vector; and $f = [f_1, f_2, \dots, f_n]^T$ are the vectors of nonlinear functions which defines the states. If the derivative of the state variable is not an explicit function of time, the system is autonomous [18]. At this point, Equation (10) can be simplified as:

$$\dot{x} = f(x, u) \quad (11)$$

Output variables are the ones which can be directly measured in power systems. They can be described by functions of state and input variables:

$$\mathbf{y} = \mathbf{g}(\mathbf{x}, \mathbf{u}) \quad (12)$$

where m is the number of the output variables; $\mathbf{y} = [y_1, y_2, \dots, y_m]^T$ is the vector of output variables; and $\mathbf{g} = [g_1, g_2, \dots, g_m]^T$ is the vector of non-linear functions which define the outputs.

In small signal analysis, a linear technique can give useful information for the intrinsic dynamic characteristics of power systems. The linearized model of Equations (11) and (12) is [23]:

$$\Delta \dot{\mathbf{x}} = \mathbf{A} \Delta \mathbf{x} + \mathbf{B} \Delta \mathbf{u} \quad (13)$$

$$\Delta \mathbf{y} = \mathbf{C} \Delta \mathbf{x} + \mathbf{D} \Delta \mathbf{u} \quad (14)$$

where \mathbf{A} is an $n \times n$ state matrix; \mathbf{B} is an $n \times r$ input matrix; \mathbf{C} is an $m \times n$ output matrix; \mathbf{D} is a feedforward matrix. The oscillation modes can be identified by the eigenvalues of state matrix \mathbf{A} [24]. Lyapunov's first law indicates that if all eigenvalues have negative real parts, the system is asymptotically stable at equilibrium point.

The real eigenvalue $\lambda_i = \alpha_i$ corresponds to a non-oscillating mode. Negative real eigenvalues ($\alpha_i < 0$) indicate a decay mode. The larger the amplitude, the faster the decay. Positive eigenvalues ($\alpha_i > 0$) indicate non-periodic instable modes. The complex eigenvalues appear as conjugation pairs $\lambda_i = \alpha_i + j\beta_i$, and each pair corresponding to one OM. The real part is related to the damping ratio ζ_i , which is defined as [25]:

$$\zeta_i = \frac{-\alpha_i}{\sqrt{\alpha_i^2 + \omega_i^2}} \quad (15)$$

The negative real part means damped oscillation, and the positive real part means instable OM [24]. The decay rate of the oscillation amplitude is determined by the damping ratio ζ_i . The time constant of amplitude decay is $1/|\alpha_i|$. Because ζ_i embodies the changes of the real and imaginary parts of the eigenvalues, it is considered a more appropriate measurement of the degree of the oscillation damping than α_i which only considers the changes of the real parts. The mode corresponding to each critical eigenvalue which satisfies the requirements can represent different types of oscillation. The imaginary part β_i is related to the oscillation frequency of the OMs.

3.3. The Index of Best Buses Selection

After performing modal analysis for all the random scenarios, the oscillation characteristics of OMs can be obtained for further analysis. The probabilistic critical OMs (PCOM) should be identified first. PCOM is defined as the OMs whose probability of being poorly damped exceeds 50%:

$$S_{pcom} = \{i | P(0 \leq \zeta_i \leq 0.05) > 50\%, i = 1 \dots N_{om}\} \quad (16)$$

where S_{pcom} represents the set of PCOMs, N_{om} is the number of OMs, $P(\cdot)$ means probability, which can be calculated by:

$$P(0 \leq \zeta_i \leq 0.05) = \frac{1}{N} \sum_{m=1}^N R_{im} \quad (17)$$

$$R_{im} = \begin{cases} 1, \zeta_{im} > 0.05 \\ 0, \zeta_{im} < 0.05 \end{cases}$$

where R_{im} represents the damping state of i th OM in m th scenario.

Then the probabilistic controllability indices of all the potential buses can be calculated. The controllability index reflects the influence of input variables on OMs. Since the main aim of the AC/DC interconnection system systems is power transmission, the element of input vector \mathbf{u} is the injection power at different buses. The controllability index is defined as:

$$CI_{ob}^s = |v_o^s B_b^s| \quad (18)$$

where CI_{ob} is the magnitude of the products of v_o and B_b , v_o represents the o th left eigenvector, and B_b is the b th column of input matrix B . Superscript s represents the s -th operation scenario. CI_{ob} evaluates the controllability of the power injected at bus b for o th mode. CI_o evaluates the controllability of the power injected at all buses for o th mode. CI is updated as [26]:

$$CI_{ob}^s = CI_{ob}^s / \max CI_o^s \quad (19)$$

where $\max CI_o^s$ is the maximum CI_{ob} out of all locations on the s -th operation scenario.

Then average value μ_{ob} and variance σ_{ob}^2 can be calculated by:

$$\begin{aligned} \mu_{ob} &= \frac{1}{M} \sum_{m=1}^M C_{ob}^m \\ \sigma_{ob}^2 &= \frac{1}{M} \sum_{m=1}^M (C_{ob}^m - \mu_{ob})^2 \end{aligned} \quad (20)$$

The best locations can be selected as the ones which has the highest μ_{ob} and $\sigma_{ob}^2 < \sigma_{\max}^2$.

3.4. The Process of Probabilistic Small Signal Stability Analysis (PSSSA) and Location Selection

The flow chart of proposed method is shown in Figure 2. The detailed processes are as follows:

- (1) Set the total sample number N ;
- (2) Generate random load and generator's output by the LHS method;
- (3) The DC system is equivalent to a -100 MW load. The -100 MW load is regarded as a mobile load. Put the mobile load and a breaker to one bus in once simulation;
- (4) Calculate the power flow and perform modal analysis. Get the matrices A , B and C from DIgSILENT/PowerFactory;
- (5) Repeat steps 3 and 4 on each bus under the same load level;
- (6) Repeat steps 2–4 until N is satisfied;
- (7) Select the critical oscillation modes by analysing the damping ratio and system's frequency under different modes. Calculate the controllability index of all buses on critical OMs;
- (8) Calculate the controllability index matrix and select the bus with the maximum probability of maximal controllability index value as the best DC terminal.

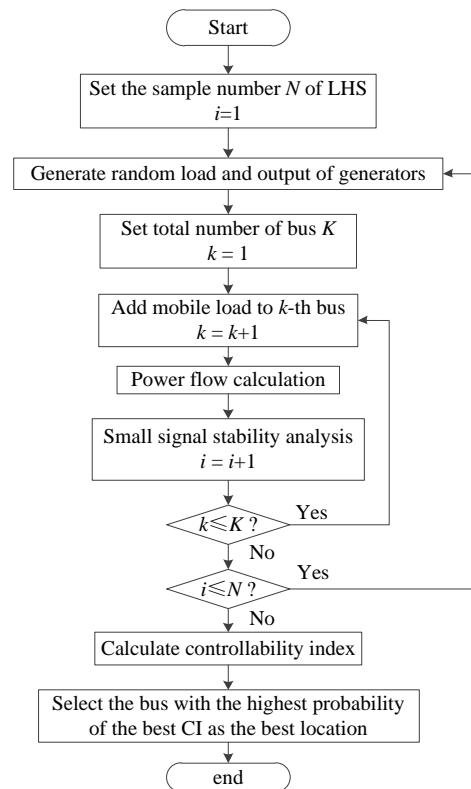


Figure 2. Flow chart of proposed method.

4. Case Study

The proposed method is applied in the IEEE 39-bus system. The result of modal analysis is obtained by the Modal Analysis Package of DIGSILENT/PowerFactory. The random load of the system is assumed to follow the normal distribution. The expected value and the variance of loads are $P_{10,i}$ and $0.1P_{10,i}$. The output of generator changes according to the load level; 1000 random operating scenarios are generated by the LHS method.

For the test system, there are 9 poorly damped low frequency oscillation (LFO) modes. The probability of these modes is shown in Table 1. A box plot of their damping ratio is shown in Figure 3.

Table 1. The damping ratio and the probability of LFO modes.

Mode	Original System Data		Probability	
	Frequency (Hz)	Damping Ratio	$\zeta < 0.05$	$\zeta < 0.1$
Mode 1	1.45	0.089	0	99.80%
Mode 2	1.423	0.078	0	99.50%
Mode 3	1.411	0.083	0	100%
Mode 4	1.196	0.062	0	100%
Mode 5	1.19	0.077	0.20%	100%
Mode 6	1.114	0.041	99.80%	100%
Mode 7	1.053	0.058	0	100%
Mode 8	0.979	0.068	0	100%
Mode 9	0.639	0.078	0	78.60%

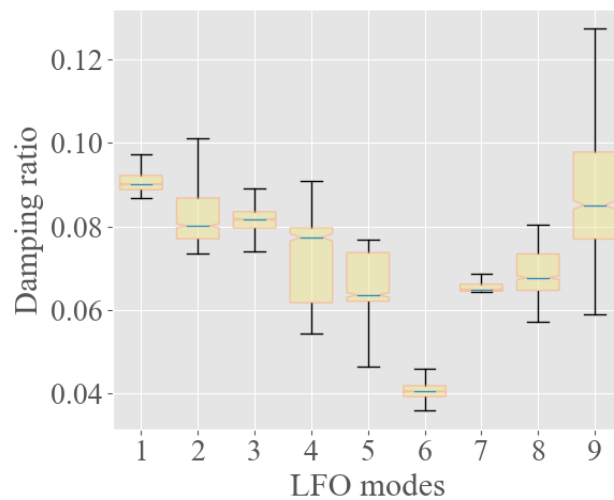


Figure 3. Box plot of damping ratio of LFO modes.

According to Table 1, only OM 6 is considered to be the probabilistic critical OM. Other OMs whose damping ratio is most likely lower than 0.1 can be included in S_{pcom} . Thus, $S_{pcom} = \{OM\ 3, OM\ 4, OM\ 5, OM\ 6, OM\ 7, OM\ 8\}$. The mean values of the mode controllability for S_{pcom} are shown in Table 2.

Table 2. Mean value of controllability indices of buses to different oscillatory modes (OMs).

Bus	OM					
	3	4	5	6	7	8
1	0.963	0.980	0.981	0.979	0.984	0.984
2	0.904	0.950	0.951	0.944	0.959	0.957
3	0.911	0.927	0.930	0.956	0.939	0.952
...
9	0.980	0.972	0.960	0.991	0.972	0.980
10	0.945	0.911	0.863	0.978	0.920	0.939
11	0.945	0.914	0.869	0.977	0.920	0.940
...
19	0.918	0.856	0.924	0.975	0.904	0.968
20	0.924	0.830	0.919	0.974	0.894	0.970
21	0.869	0.871	0.916	0.971	0.912	0.962
...
29	0.928	0.956	0.965	0.956	0.912	0.879
30	0.907	0.959	0.956	0.906	0.977	0.960
31	0.970	0.908	0.816	0.984	0.868	0.894
...
37	0.825	0.970	0.971	0.954	0.971	0.960
38	0.941	0.969	0.976	0.958	0.902	0.851
39	1.000	1.000	1.000	1.000	1.000	1.000

It can be observed from Table 2 that the top three buses are bus39, bus1 and bus9 which are sorted by the mean value of controllability index and the probability of 6 modes. The variance of these three buses is not the maximum among all buses. Thus, the multi-infeed HVDC system is considered to be connected to the bus39, bus1 and bus9. The box plots of controllability index results from modal analysis on critical modes are shown in Figure 4. A total of 39 buses were observed.



Figure 4. Box plot of controllability index of LFO modes. (a) OM3; (b) OM4; (c) OM5; (d) OM6; (e) OM7; (f) OM8.

From Figure 4, the box plot area of bus39, bus1 and bus9 is smaller than other buses, which indicates that the controllability index distribution of the three buses is relatively concentrated. The value of these three buses’ controllability index are closer to 1 than other buses. It can be seen the result of box plots and mean value table are same. Thus, Bus39, bus1 and bus9 are the selected location.

To demonstrate the damping performance of the HVDC system, a three-phase fault is caused on the transmission line 14–15 of the 39-bus system at $t = 1$ s and lasts for 0.1 s. The simulation results are shown in Figure 5. Case 1: one HVDC system connects to bus39; Case 2: two HVDC systems connect to bus39 and bus1; Case 3: three HVDC systems connect to bus39, bus1 and bus39.

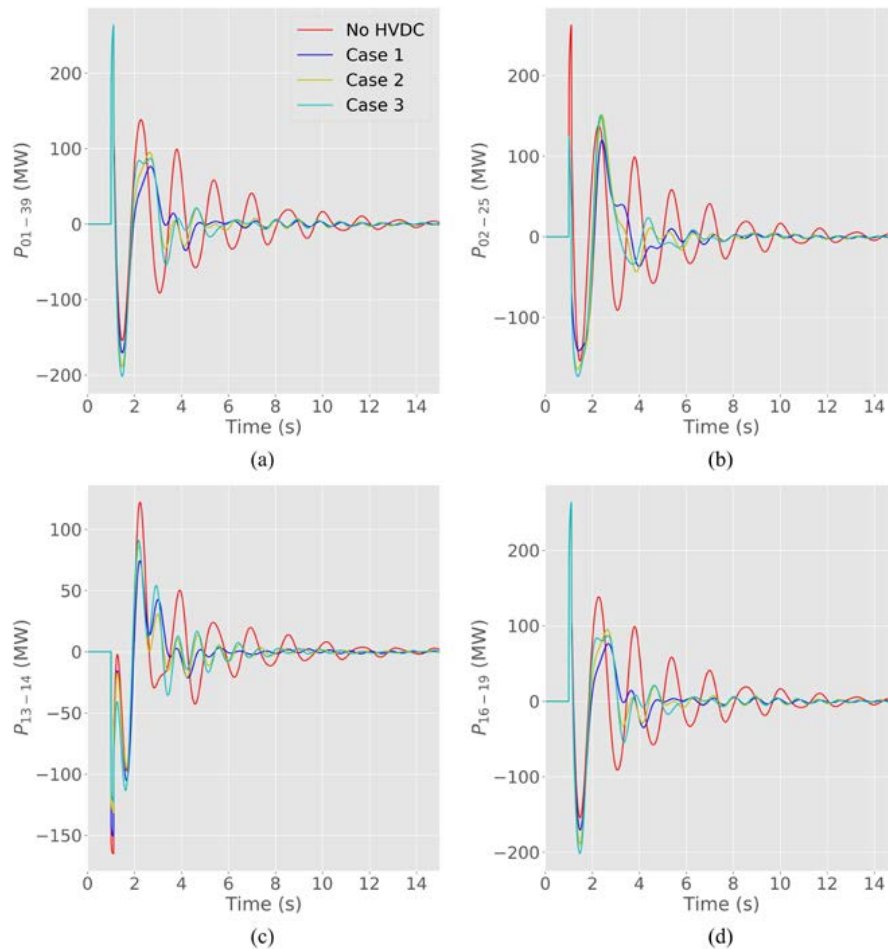


Figure 5. The power oscillations on transmission lines. (a) Line 01–39; (b) Line 02–25; (c) Line 13–14; (d) Line 16–19.

It can be observed from Figure 5 that the HVDC system has the effective damping performance. When there is no HVDC to be connected, the oscillations last for long time. When bus39 connects with one HVDC system, the oscillations time decreases significantly. When the candidate three buses all connect with HVDC systems, it takes less time to return to the equilibrium point. The dynamic response of the rotor angular velocity can be shown by Figure 6.

Figure 6 shows that the system connected with HVDC system can have better damping effect than there is no HVDC to be connected. When the three buses all connect with HVDC systems, the system has the best damping effect.

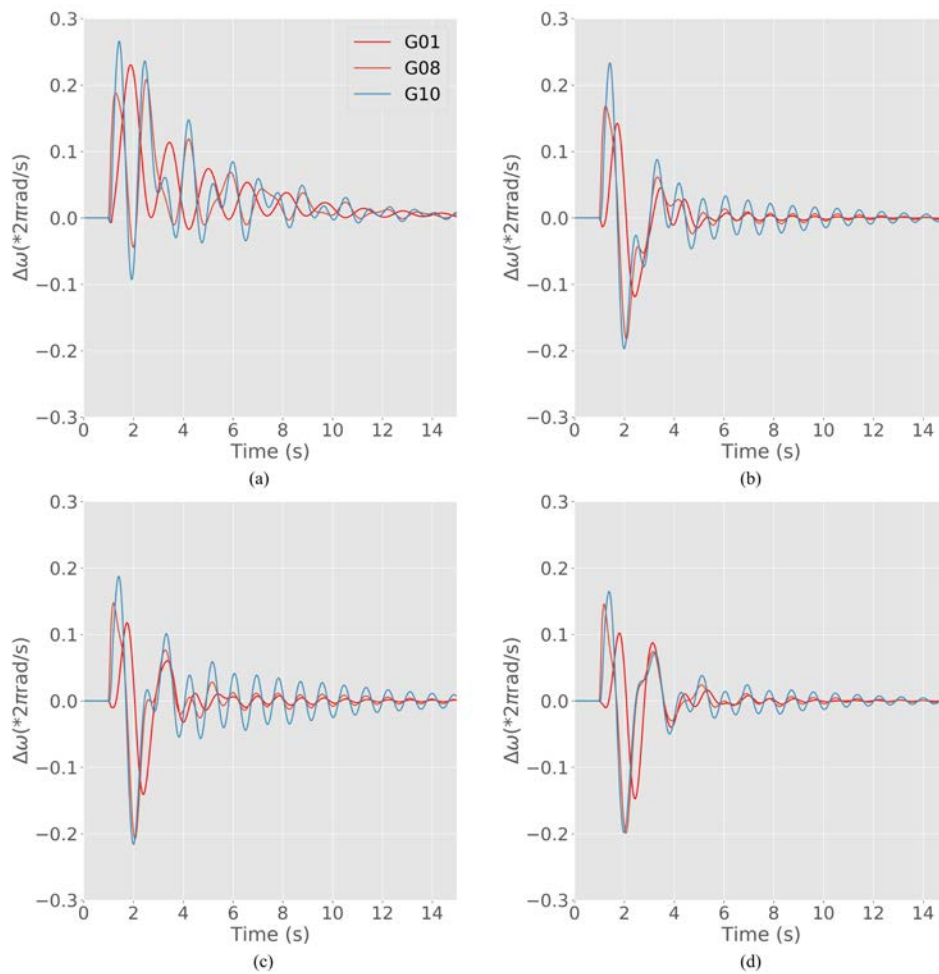


Figure 6. The deviation and the derivative of ω . (a) No high-voltage direct current (HVDC); (b) Case 1; (c) Case 2; (d) Case 3.

5. Discussion

By contrast with the previous location selection method of HVDC systems, the proposed method mainly focusses on the impact of the locations on system stability. In [5,6], the best locations of HVDC links in 39-bus systems are identified as {bus3, bus22, bus35} and {bus8, bus20, bus27}, respectively. To compare the system dynamic responses with different HVDC locations, three cases are set: (1) Case A: the locations selected by this paper {bus1, bus9, bus39}; (2) Case B: the locations found by [5], i.e., {bus3, bus22, bus35}; (3) Case C: the locations found by [6], i.e., {bus8, bus20, bus27}. A three-phase fault is applied on the transmission line L14–15 at $t = 1$ s and lasts for 0.1 s. The system dynamics responses are shown in Figure 7. Since the power flow with different HVDC locations is different, only the power deviation of the transmission lines after the disturbance are shown. It can be observed that the locations identified by this paper, i.e., Case A, has the best damping performance. The locations in [5,6] has little influence on the power oscillations as the aim of these locations are cost reduction and power flow controllability.

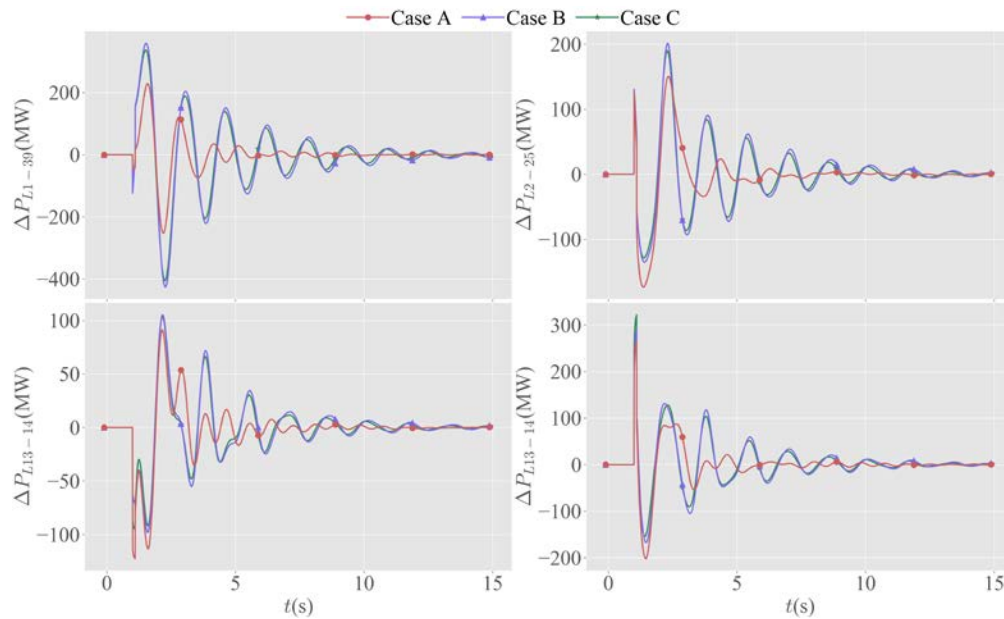


Figure 7. The transmission line power deviation with different HVDC locations.

The grid losses are summarized in Table 3. One can observe that the grid losses with the HVDC locations identified in [5,6] are lower than with the locations selected in this paper. Although the grid losses are increased, the stability of the hybrid AC/DC power system is improved.

Table 3. Grid losses with different HVDC locations.

Case	Location	Grid Losses
Without HVDC	None	43.71 MW
A	bus1, bus9, bus39	48.82 MW
B	bus3, bus22, bus35	43.69 MW
C	bus8, bus20, bus27	47.21 MW

6. Conclusions

In this paper, a probabilistic small signal stability assessment methodology based on the Latin hypercube sampling-based Monte Carlo simulation approach has been proposed. The heavy computation burden of the traditional MC method is significantly decreased by the LHS technique. The influence of potential locations of HVDC systems on the system stability is studied in a probabilistic way. The probabilistic critical oscillatory modes are identified and the candidates of the potential locations of multi-infeed HVDC systems can be distinguished by the probabilistic controllability index to improve the system damping performance. This method can be used for the initial selection of the scheme of arbitrary locations of the HVDC station in the planning stage. The effectiveness of the selected candidate locations is validated by the non-linear time-domain simulations in DIgSILENT/PowerFactory. Compared with other methods, the locations identified by the proposed method can effectively improve the stability of the hybrid AC/DC power system. The results show that the system damping to the probabilistic critical modes are enhanced and the power oscillations on the transmission lines are suppressed effectively. However, the grid losses are slightly magnified. Thus, in our future work, both the economic factors and the stability factors will be considered in the HVDC placement tasks.

Author Contributions: Conceptualization, X.L. and Y.L. (Yunfeng Li); methodology, Y.L. (Yong Li) and Y.C.; software, W.W. and L.L.; validation, L.L. and W.W.; formal analysis, X.L. and Y.L. (Yunfeng Li); investigation, Y.L. (Yong Li); resources, W.W.; data curation, L.L.; writing—original draft preparation, L.L.; writing—review and editing, L.L. and W.W.; visualization, L.L. and W.W.; supervision, Y.L. (Yong Li); project administration, Y.L.

(Yunfeng Li); funding acquisition, Y.L. (Yunfeng Li). All authors have read and agreed to the published version of the manuscript.

Funding: This research was funded by Science and Technology Project of State Grid Hunan Electric Power Limited Company, grant number 5216A218000B.

Conflicts of Interest: The authors declare no conflict of interest.

Nomenclature

HVDC	High Voltage Direct Current
PSSSA	Probabilistic Small Signal Stability Assessment
LHS-MCS	Latin Hypercube Sampling-based Monte Carlo Simulation
OM	Oscillation Mode
SSSA	Small Signal Stability Analysis
MC	Monte Carlo
LHS	Latin Hypercube Sampling
SRS	Simple Random Sampling
PDF	Probability Density Function
CPDF	Cumulative Probability Density Function
PCOM	Probabilistic Critical Oscillation Mode
DC	Direct Current
AC	Alternating Current

References

1. Aik, D.L.H.; Andersson, G. Power stability analysis of multi-infeed HVDC systems. *IEEE Trans. Power Deliv.* **1998**, *13*, 923–931. [[CrossRef](#)]
2. Guo, X.J.; Ma, S.Y.; Bu, G.Q.; Tang, Y. Survey on coordinated control of multi-infeed DC systems. *Autom. Electr. Power Syst.* **2009**, *33*, 9–15.
3. Chatzivasilieadis, S.; Krause, T.; Andersson, G. HVDC line placement for maximizing social welfare—An analytical approach. In Proceedings of the 2013 IEEE Grenoble Conference, Grenoble, France, 16–20 June 2013; pp. 1–6.
4. Bucher, M.A.; Wiget, R.; Perez, G.H.; Andersson, G. Optimal placement of multi-terminal HVDC interconnections for increased operational flexibility. In Proceedings of the 2014 5th IEEE PES Innovative Smart Grid Technologies, Istanbul, Turkey, 12–15 October 2014; pp. 1–6.
5. Franken, M.; Barrios, H.; Schirief, A.B.; Puffer, R. Identification of suitable locations for HVDC links within meshed AC networks. In Proceedings of the 2019 IEEE PES Innovative Smart Grid Technologies Europe (ISGT-Europe), Bucharest, Romania, 29 September–2 October 2019; pp. 1–5.
6. Giuntoli, M.; Schmitt, S.; Biagini, V.; Subasic, M.; Gutermuth, G.; Krontiris, A. Placement of HVDC links for reduction of network congestions. In Proceedings of the 2019 AEIT HVDC International Conference, Florence, Italy, 9–10 May 2019; pp. 1–6.
7. Guo, X.J.; Guo, J.B.; Ma, S.Y.; Wang, C.S.; Zhang, Y.T. A method for multi DC terminal location selection based on multi-infeed short circuit ratio. *Proc. CSEE* **2013**, *33*, 36–42.
8. Zhou, Q.Y.; Liu, Y.T.; Tang, Y. A method to select terminal locations in multi-infeed HVDC power transmission system considering weights of HVDC transmission lines. *Power Syst. Technol.* **2013**, *37*, 3336–3341.
9. Xue, Y.S.; Liu, Q.; Dong, Z.Y.; Ledwich, G.; Yuan, Y. A review of non-deterministic analysis for power system transient stability. *Autom. Electr. Power Syst.* **2007**, *31*, 1–6.
10. Liu, S.; Liu, P.X.; Wang, X. Stochastic small-signal stability analysis of grid-connected photovoltaic systems. *IEEE Trans. Ind. Electron.* **2016**, *63*, 1027–1038. [[CrossRef](#)]
11. Burchett, R.C.; Heydt, G. Probabilistic methods for power system dynamic stability studies. *IEEE Trans. Power Appar. Syst.* **1978**, *97*, 695–702. [[CrossRef](#)]
12. Huang, H.Z.; Chung, C.Y.; Chan, K.W.; Chen, H.Y. Quasi-Monte Carlo based probabilistic small signal stability analysis for power systems with plug-in electric vehicle and windpower integration. *IEEE Trans. Power Syst.* **2013**, *28*, 3335–3343. [[CrossRef](#)]

13. Rueda, J.L.; Colome, D.G.; Erlich, I. Assessment and enhancement of small signal stability considering uncertainties. *IEEE Trans. Power Syst.* **2009**, *24*, 198–207. [[CrossRef](#)]
14. Bu, S.Q.; Du, W.; Wang, H.F.; Chen, Z.; Xiao, L.Y.; Li, H.F. Probabilistic analysis of small-signal stability of large-scale power systems as affected by penetration of wind generation. *IEEE Trans. Power Syst.* **2012**, *27*, 762–770. [[CrossRef](#)]
15. Xu, Z.; Dong, Z.Y.; Zhang, P. Probabilistic small signal analysis using Monte Carlo simulation. In Proceedings of the IEEE Power Engineering Society General Meeting, San Francisco, CA, USA, 16 June 2005.
16. McKay, M.D.; Conover, W.J.; Beckman, R.J. A comparison of three methods for selecting values of input variables in the analysis of output from a computer code. *Technometrics.* **1979**, *21*, 55–61.
17. Cai, D.F.; Shi, D.Y.; Chen, J.F. Probabilistic load flow computation using Copula and Latin hypercube sampling. *IET Gener. Transm. Distrib.* **2014**, *8*, 1539–1549. [[CrossRef](#)]
18. Helton, J.C.; Davis, F.J. Latin hypercube sampling and the propagation of uncertainty in analyses of complex systems. *Reliab. Eng. Syst. Saf.* **2003**, *81*, 23–69. [[CrossRef](#)]
19. Da Silva, A.M.L.; Ribeiro, S.M.P.; Arienti, V.L.; Allan, R.N.; Do Coutto Filho, M.B. Probabilistic load flow techniques applied to power system expansion planning. *IEEE Trans. Power Syst.* **1990**, *5*, 1047–1053. [[CrossRef](#)]
20. Yu, H.; Chung, C.Y.; Wong, K.P.; Lee, H.W.; Zhang, J.H. Probabilistic load flow evaluation with hybrid latin hypercube sampling and cholesky decomposition. *IEEE Trans. Power Syst.* **2009**, *24*, 661–667. [[CrossRef](#)]
21. Silva-Saravia, H.; Wang, Y.; Pulgar-Painemal, H. Determining wide-area signals and locations of regulating devices to damp inter-area oscillations through eigenvalue sensitivity analysis using DlgSILENT programming language. In *Advanced Smart Grid Functionalities Based on PowerFactory*; Green Energy and Technology; Springer: Cham, Switzerland, 2018; pp. 153–179.
22. Kundur, P. Small signal stability. In *Power System Stability and Control*; McGraw-Hill: New York, NY, USA, 1994; pp. 465–471.
23. Wang, W.Y.; Li, Y.; Cao, Y.J.; Ulf, H.; Christian, R. Adaptive droop control of VSC-MTDC system for frequency support and power sharing. *IEEE Trans. Power Syst.* **2018**, *33*, 1264–1274. [[CrossRef](#)]
24. Dong, Z.Y.; Pang, C.K.; Zhang, P. Power system sensitivity analysis for probabilistic small signal stability assessment in a deregulated environment. *Int. J. Control Autom. Syst.* **2005**, *3*, 355–362.
25. Wang, K.W.; Chung, C.Y.; Tse, C.T.; Tsang, K.M. Improved probabilistic method for power system dynamic stability studies. *Proc. Inst. Elect. Eng. Gen. Transm. Distrib.* **2000**, *147*, 37–43. [[CrossRef](#)]
26. Silva-Saravia, H.; Pulgar-Painemal, H.; Mauricio, J. Flywheel energy storage model, control and location for improving stability: The Chilean case. *IEEE Trans. Power Syst.* **2017**, *32*, 3111–3119. [[CrossRef](#)]



© 2020 by the authors. Licensee MDPI, Basel, Switzerland. This article is an open access article distributed under the terms and conditions of the Creative Commons Attribution (CC BY) license (<http://creativecommons.org/licenses/by/4.0/>).